Preprints.org

Article

Not peer-reviewed version

Two Farm-Structured Azoxystrobin Phenotypes and No In Vitro Copper Activity in *Moniliophthora roreri* from the Ecuadorian Amazon

Pablo Israel Alvarez-Romero *, Ana Francisca Tibúrcia Amorim Ferreira e Ferreira , Daniel Arturo Román-Robalino , Vanesa Belén Morales-León , Nicole Carolina Torres-Revelo , Hamiltón Octavio Intriago-Reina

Posted Date: 17 November 2026

Keywords: frosty pod rot; *Theobroma cacao*; EC_{50}; baseline sensitivity; QoI fungicides; azoxystrobin; copper; population structure; principal component analysis; Monte Carlo simulation

Preprints.org is a free multidisciplinary platform providing preprint service that is dedicated to making early versions of research outputs permanently available and citable. Preprints posted at Preprints.org appear in Web of Science, Crossref, Google Scholar, Scilit, Europe PMC, OpenAlex.

Copyright: This open access article is published under a Creative Commons CC BY 4.0 license, which permit the free download, distribution, and reuse, provided that the author and preprint are cited in any reuse.

Preprints.org | NOT PEER-REVIEWED | Posted: 17 November 2026 https://doi.org/10.20944/preprints202611.1684.v1

Disclaimer/Publisher's Note: The statements, opinions, and data contained in all publications are solely those of the individual author(s) and contributor(s) and not of MDPI and/or the editor(s). MDPI and/or the editor(s) disclaim responsibility for any injury to people or property resulting from any ideas, methods, instructions, or products referred to in the content.

Article

Two Farm-Structured Azoxystrobin Phenotypes and No In Vitro Copper Activity in *Moniliophthora roreri* from the Ecuadorian Amazon

Pablo Israel Alvarez-Romero [1,*], Ana Francisca Tibúrcia Amorim Ferreira e Ferreira [2], Daniel Arturo Román-Robalino [1], Vanesa Belén Morales-León [1], Nicole Carolina Torres-Revelo [3] and Hamiltón Octavio Intriago-Reina [1]

[1] Escuela Superior Politécnica de Chimborazo (ESPOCH), Panamericana Sur Km 1 ½, Riobamba 060155, Ecuador

[2] Programa de Pós-Graduação em Agronomia Tropical, Federal University of Amazonas, Manaus 69067-005, Brazil

[3] Independent Researcher, Riobamba, Ecuador

* Correspondence: pabloi.alvarez@espoch.edu.ec

Abstract

Frosty pod rot, caused by *Moniliophthora roreri*, is the main disease of cacao in the Ecuadorian Amazon, where fungicide use is rising without sensitivity baselines. We measured the mycelial growth of 23 single-spore isolates from six farms in Orellana Province on media amended with azoxystrobin, boscalid, difenoconazole or copper sulfate (0.01–100 μg mL^{-1}) and estimated EC_{50} values. Difenoconazole was the most active (geometric mean 0.32 μg mL^{-1}). Boscalid gave a narrow distribution (1.02 μg mL^{-1}) apart from three slow-growing isolates. Copper sulfate did not halve the growth of any isolate at 100 μg mL^{-1}. Azoxystrobin split the collection into 11 sensitive isolates (0.035 μg mL^{-1}) and 12 less sensitive ones (1.00 μg mL^{-1}), with none in between (mixture model, $p = 0.002$). The less sensitive isolates came mostly from a commercial CCN51 farm and a Nacional farm, and isolates from the same field sample behaved alike. A principal component analysis of the growth profiles, run without prior grouping, placed azoxystrobin on the first axis (35.1% of the variance). Twenty-three isolates suffice as provisional baselines for difenoconazole and boscalid; azoxystrobin needs about 120 farm-stratified isolates to detect a threefold shift. These are in vitro phenotypes; resistance has not been demonstrated.

Keywords: frosty pod rot; *Theobroma cacao*; EC_{50}; baseline sensitivity; QoI fungicides; azoxystrobin; copper; population structure; principal component analysis; Monte Carlo simulation

1. Introduction

Frosty pod rot attacks the fruit of cacao (*Theobroma cacao* L.). Its agent, the basidiomycete *Moniliophthora roreri* (Cif.) H.C. Evans, Stalpers, Samson & Benny, infects pods while they are small and stays latent for several weeks. Then the pods rot and become covered by a cream-coloured mat of spores [1–3]. One diseased pod releases enormous numbers of spores, wind and rain carry them to the next cohort of fruits, and in unmanaged plantings the disease can take most of the harvest [1,2]. The fungus belongs to the Marasmiaceae, next to *M. perniciosa*, which causes witches' broom [4].

For most of the twentieth century the pathogen stayed in north-western South America. It has since reached Central America, Mexico, Peru and Bolivia, and its spread has followed the expansion of cacao growing closely [1,5]. Its genetic diversity peaks in Colombia [6]. Cacao was first used and domesticated in the upper Amazon of south-eastern Ecuador about 5300 years ago [7], and that region still holds much of the genetic variation of the species [8]. Orellana Province lies in its northern part. Cacao is now one of the province's main cash crops, grown as the fine-flavour Nacional type,

© 2026 by the author(s). Distributed under a Creative Commons CC BY license.

Preprints.org | NOT PEER-REVIEWED | Posted: 17 November 2026 https://doi.org/10.20944/preprints202611.1684.v1

the high-yielding clone CCN51 and a local selection called Súper Árbol, and frosty pod rot is present in all of them [9].

Growers still rely mostly on cultural control. They remove diseased pods at short intervals and regulate shade and prune to lower inoculum and canopy humidity [2,10,11]. Many smallholders cannot pay for that much labour, so they turn to fungicides, traditionally copper. In Mexico, one application of azoxystrobin, trifloxystrobin, tebuconazole or propiconazole combined with monthly copper hydroxide sprays reduced disease incidence in the field [12]. In Ecuador, azoxystrobin and copper sulfate have been tested in vitro and in spray programmes [13,14].

Single-site fungicides carry a cost. The Fungicide Resistance Action Committee (FRAC) rates the quinone outside inhibitors (QoIs, FRAC group 11) as high-risk, the succinate dehydrogenase inhibitors (SDHIs, group 7) as medium- to high-risk and the demethylation inhibitors (DMIs, group 3) as medium-risk [15,16]. To manage that risk one needs to know how sensitive the population was before selection began, which means a baseline distribution against which later samples can be compared [17,18]. For *M. roreri* such data are thin. The largest survey so far tested 76 Ecuadorian isolates against azoxystrobin and found all of them highly sensitive [19]. Another Ecuadorian study used two isolates [13]. We found no population data for an SDHI or a DMI, and no study that tested several modes of action on the same Amazonian isolates.

A list of EC_{50} values does not make a baseline by itself. *M. roreri* reproduces clonally [20], so isolates from the same pod, tree or farm may be copies of one clone, and a collection can look larger than it is. If sensitivity differs among farms, a provincial mean can hide a subpopulation that has already shifted.

We set out to describe the in vitro sensitivity of 23 *M. roreri* isolates from Orellana Province to azoxystrobin, boscalid, difenoconazole and copper sulfate, working from the full plate-level growth data. We also tested whether sensitivity was structured by farm, canton or cacao genotype, and used resampling and simulation to estimate how many isolates a baseline for each fungicide would need.

2. Materials and Methods

2.1. Study Area and Isolates

The isolates came from the three cantons of Orellana Province, Ecuador, and were sampled in the same project as our survey of cacao fruit endophytes [9]. Loreto lies at 0°47′28″ S, 77°22′19″ W and 373 m a.s.l. (mean temperature 23.6 °C, relative humidity 81–89%, annual rainfall 2516 mm), Francisco de Orellana at 0°37′36″ S, 77°07′40″ W and 292 m a.s.l. (26 °C; 86–89%; 2800–4500 mm), and La Joya de los Sachas at 0°45′41″ S, 77°05′01″ W and 330 m a.s.l. (25 °C; 90%; 4534 mm). Pods with symptoms of frosty pod rot were collected in five sampling rounds between June 2021 and May 2022 on six farms (Table 1). La Belleza is in Francisco de Orellana, and La Paz and Bajo Huiruno are in the parish of Puerto Murialdo. La Calumeña (Lago San Pedro), Unión Milagreña and San Carlos (parish of San Carlos) are in Joya de los Sachas. The trees were CCN51, Súper Árbol or Nacional. The isolates were obtained from the symptomatic pods collected on these farms at the Plant Pathology Laboratory of the Escuela Superior Politécnica de Chimborazo (ESPOCH), Riobamba, where they were also characterized and assayed.

Spores were taken from sporulating lesions with a sterile syringe and plated on potato dextrose agar (PDA; 39 g L^{-1}; Difco, Becton, Dickinson and Company, Franklin Lakes, NJ, USA), which was incubated at 28 °C in the dark. After 10 days, colonies were purified by successive transfers until single-spore cultures were obtained. These were preserved in sterile distilled water by the Castellani method at 4–8 °C [9,21]. Isolates were identified from symptoms, culture characters and morphology. Diseased pods showed the internal necrosis and cream-coloured sporulating mat typical of frosty pod rot [1,2]. Colonies were described by mycelial colour on the obverse and reverse, recorded with the Pantone Color Matching System, and by margin shape, texture and elevation. Adhesive-tape mounts in lactoglycerol [22], examined under a Leica DML microscope, showed chains of globose to ellipsoid spores [2,3]. No molecular identification was performed.

© 2026 by the author(s). Distributed under a Creative Commons CC BY license.

Preprints.org | NOT PEER-REVIEWED | Posted: 17 November 2026 https://doi.org/10.20944/preprints202611.1684.v1

Twenty-three isolates (C1–C23) were retained. Thirteen came from Joya de los Sachas, 8 from Francisco de Orellana and 2 from Loreto; 9 were from CCN51, 8 from Súper Árbol and 6 from Nacional trees. Seven pairs of isolates shared a field sample, so the collection represents 16 field samples, and the analysis took the pairing into account (Section 2.6).

Table 1. Origin of the 23 *Moniliophthora roreri* isolates (Orellana Province, Ecuador). Isolates whose field codes share a sample prefix (e.g., O-FO-03) came from the same field sample.

Isolate	Field code	Canton	Parish	Farm	Cacao genotype	Sampling date
C1	OL-P-07-A1	Loreto	Puerto Murialdo	La Paz	CCN51	18 Oct 2021
C2	O-FO-05-A3	F. de Orellana	La Belleza	La Belleza	CCN51	17 Aug 2021
C3	OS-LS-03-A1	J. de los Sachas	Lago San Pedro	La Calumeña	Súper Árbol	16 Jun 2021
C4	OS-UM-03-A1	J. de los Sachas	Unión Milagreña	Unión Milagreña	Súper Árbol	16 Jun 2021
C5	JS-SC-A1	J. de los Sachas	San Carlos	San Carlos	Nacional	Oct 2021
C6	OL-09-A1	F. de Orellana[a]	Puerto Murialdo	Bajo Huiruno	CCN51	18 Jan 2022
C7	OS-UM-09-A1	J. de los Sachas	Unión Milagreña	Unión Milagreña	Nacional	21 Jan 2022
C8	OS-SC-03-A1	J. de los Sachas	San Carlos	San Carlos	Nacional	18 Jun 2021
C9	OS-LS-05-A3	J. de los Sachas	Lago San Pedro	La Calumeña	Súper Árbol	20 Aug 2021
C10	OL-03-A1	Loreto	Puerto Murialdo	La Paz	Súper Árbol	16 Jun 2021
C11	OS-LS-09-A3	J. de los Sachas	Lago San Pedro	La Calumeña	Súper Árbol	21 Jan 2022
C12	OS-LS-05-A2	J. de los Sachas	Lago San Pedro	La Calumeña	Súper Árbol	20 Aug 2021
C13	OS-LS-09-A1	J. de los Sachas	Lago San Pedro	La Calumeña	Súper Árbol	21 Jan 2022
C14	O-FO-09-A2	F. de Orellana	La Belleza	La Belleza	CCN51	18 Jan 2022
C15	OS-SC-03-A2	J. de los Sachas	San Carlos	San Carlos	Nacional	18 Jun 2021
C16	OS-SC-05-A1	J. de los Sachas	San Carlos	San Carlos	Nacional	20 Aug 2021
C17	OS-SC-09	J. de los Sachas	San Carlos	San Carlos	Nacional	21 Jan 2022
C18	O-FO-03-A1	F. de Orellana	La Belleza	La Belleza	CCN51	16 Jun 2021
C19	O-FO-05-A1	F. de Orellana	La Belleza	La Belleza	CCN51	17 Aug 2021
C20	O-FO-03-A2	F. de Orellana	La Belleza	La Belleza	CCN51	16 Jun 2021
C21	O-FO-09-A1	F. de Orellana	La Belleza	La Belleza	CCN51	18 Jan 2022
C22	OS-UM-03-A2	J. de los Sachas	Unión Milagreña	Unión Milagreña	Súper Árbol	16 Jun 2021
C23	O-FO-MF-05	F. de Orellana	La Belleza	La Belleza	CCN51	6 May 2022

F. de Orellana, Francisco de Orellana; J. de los Sachas, Joya de los Sachas. Totals: Joya de los Sachas 13, Francisco de Orellana 8 and Loreto 2 isolates; CCN51 9, Súper Árbol 8 and Nacional 6. Same-sample pairs: C2/C19, C4/C22, C8/C15, C9/C12, C11/C13, C14/C21 and C18/C20. [a] Canton as given in the collection record and the laboratory data sheet; the community of Bajo Huiruno lies in Loreto according to field records and ref. [9].

2.2. Fungicides and Amended Media

Four fungicides with different modes of action were tested (Table 2) [15]. They were azoxystrobin (QoI; FRAC group 11), boscalid (SDHI; group 7), difenoconazole (DMI; group 3) and copper sulfate, used as copper sulfate pentahydrate ($CuSO_4 \cdot 5H_2O$; inorganic multisite; group M01). All four were commercial products: Amistar® 50 WG (azoxystrobin 500 g kg^{-1}, water-dispersible granules; Syngenta, Basel, Switzerland), Cantus® (boscalid 500 g kg^{-1}, WG; BASF, Ludwigshafen, Germany), Score® 250 EC (difenoconazole 250 g L^{-1}, emulsifiable concentrate; Syngenta) and Phyton® 27 ($CuSO_4 \cdot 5H_2O$ 240 g L^{-1}, soluble concentrate; Phyton Corp., Bloomington, MN, USA). Concentrations refer to the active ingredient and, for copper, to the pentahydrate salt, of which metallic copper makes

© 2026 by the author(s). Distributed under a Creative Commons CC BY license.

Preprints.org | NOT PEER-REVIEWED | Posted: 17 November 2026 https://doi.org/10.20944/preprints202611.1684.v1

up about 25% (molar mass 249.7 g mol^{-1}; Cu 63.55 g mol^{-1}). A stock solution of 10 000 µg mL^{-1} of active ingredient (for copper, of copper sulfate pentahydrate) was prepared in sterile distilled water. It was diluted 1:2 and then serially 1:10 to obtain working solutions of 5000, 500, 50, 5 and 0.5 µg mL^{-1}. Following Mihajlović et al. [23], 0.918 mL of the corresponding working solution was added to 45 mL of molten PDA to give final concentrations of 100, 10, 1, 0.1 and 0.01 µg mL^{-1}. Fifteen millilitres were dispensed into each of three 90 mm Petri dishes per concentration. Control plates (0 µg mL^{-1}) were prepared without fungicide.

Table 2. Fungicides evaluated, their FRAC classification [15] and the products used.

Active ingredient	Chemical group	FRAC code (target site)	Target	Resistance risk	Product (manufacturer); a.i. content, formulation
Azoxystrobin	Methoxy-acrylate (QoI)	11 (C3)	Cytochrome *bc*$_1$, Qo site (complex III)	High	Amistar® 50 WG (Syngenta); 500 g kg^{-1}, WG
Boscalid	Pyridine-carboxamide (SDHI)	7 (C2)	Succinate dehydrogenase (complex II)	Medium to high	Cantus® (BASF); 500 g kg^{-1}, WG
Difenoconazole	Triazole (DMI)	3 (G1)	Sterol C14-demethylase (CYP51)	Medium	Score® 250 EC (Syngenta); 250 g L^{-1}, EC
Copper sulfate	Inorganic copper	M01	Multisite contact activity	Low	Phyton® 27 (Phyton Corp.); $CuSO_4 \cdot 5H_2O$ 240 g L^{-1}, SL

QoI, quinone outside inhibitor; SDHI, succinate dehydrogenase inhibitor; DMI, demethylation inhibitor; WG, water-dispersible granules; EC, emulsifiable concentrate; SL, soluble concentrate. Resistance risk as rated by FRAC for the group. Contents are given per kg or L of product; Phyton® 27 contains 240 g L^{-1} of the pentahydrate salt, equivalent to about 61 g L^{-1} of metallic copper.

2.3. Mycelial Growth Assays

Each fungicide was tested as a separate experiment with all 23 isolates, six concentrations and three replicate plates per concentration. The plate was the experimental unit. Plates were sown on 17 August 2022 (azoxystrobin), 22 August (boscalid), 27 August (copper sulfate) and 12 September 2022 (difenoconazole). Mycelial discs 5.8 mm in diameter were cut with sterile drinking straws from the margin of actively growing colonies and placed on the amended plates, which were incubated in the dark at 27 ± 2 °C. Two perpendicular colony diameters were measured at 48, 72, 96 and 120 h, and growth was calculated as the mean diameter minus the disc diameter. The data set holds 6624 records, with 36 missing diameters.

Three variables were derived for each plate. The mycelial growth rate (MGR, mm day^{-1}) was the slope of a linear regression of growth on time between days 2 and 5. The area under the mycelial growth curve (AUMGC, mm·day) was computed from 48 to 120 h by the trapezoidal rule, by analogy with the area under the disease progress curve [24]. Relative AUMGC was the AUMGC of each plate as a percentage of the mean of the control plates of the same isolate.

2.4. Analysis of Growth

Differences in vigour among isolates were tested with the Kruskal–Wallis test on the AUMGC of the control plates. For each fungicide, relative AUMGC was analysed as a randomized complete block design, with concentration as the treatment and isolate as the block (n = 23), and means were separated with Tukey's HSD test (α = 0.05). The same design, with fungicide as the treatment, compared the four fungicides at each concentration; the Friedman test was run alongside as a nonparametric check. Within each isolate, a one-way ANOVA of AUMGC on concentration (three plates per concentration) followed by Tukey's test showed whether that isolate responded at all. The effects of canton and cacao genotype on relative AUMGC averaged over concentrations were examined with the Kruskal–Wallis test.

© 2026 by the author(s). Distributed under a Creative Commons CC BY license.

Preprints.org | NOT PEER-REVIEWED | Posted: 17 November 2026 https://doi.org/10.20944/preprints202611.1684.v1

2.5. EC_{50} Estimation

For each isolate and fungicide, log-logistic models were fitted to the MGR of the 18 plates with the R package drc [25]. The default was the three-parameter model with the lower limit fixed at zero (LL.3), whose parameter *e* is the EC_{50}. The four-parameter model (LL.4) replaced it when its Akaike information criterion (AIC) was at least two units lower. With LL.4 the absolute EC_{50} is reported, that is, the concentration at which the fitted curve falls to half of its upper limit. For azoxystrobin, LL.4 and the absolute EC_{50} were used for all 23 isolates, because inhibition levelled off at a partial plateau, the residual growth often seen when QoIs are tested on mycelium [26]. The 95% confidence interval of each EC_{50} was a bootstrap percentile interval. Plates were resampled with replacement within each concentration, the model was refitted 300 times, and resamples that failed to converge were discarded. The delta-method intervals from drc are reported as well (Table S1). EC_{50} values were not extrapolated. Isolates whose mean inhibition at 100 μg mL^{-1} was below 50% were recorded as >100 μg mL^{-1}, and estimates below 0.01 μg mL^{-1} as <0.01 μg mL^{-1}. Recomputing the LL.3 fits with the ec50estimator package [27] returned the same estimates for every isolate. EC_{50} values were also calculated from the 120-h diameter (Table S1).

Isolates were placed in descriptive categories adapted from Gudmestad et al. [28] and consistent with the general criterion of Edgington et al. [29]. The classes were highly sensitive (HS; EC_{50} < 1 μg mL^{-1}), sensitive (S; 1–5 μg mL^{-1}), moderately sensitive (MS; >5–20 μg mL^{-1}), low sensitivity (LS; >20–100 μg mL^{-1}) and very low sensitivity (VLS; >100 μg mL^{-1}). Gudmestad et al. called the third and fourth classes moderately and highly resistant, but they set those limits for SDHIs in *Alternaria solani*, and the limits have no validated meaning for *M. roreri*. Here they are used only as a common scale.

2.6. Population Analysis

For each single-site fungicide, $\log_{10}$ EC_{50} was described by a normal distribution fitted by maximum likelihood with interval censoring (survreg, log-normal) [30,31]. The geometric mean (GM), the geometric standard deviation (GSD) and the 95th and 99th percentiles (P95, P99) were derived from the fit. Isolates from one field sample are not independent, so 95% confidence intervals came from a cluster bootstrap that resampled the 16 field samples with replacement (1000 replicates) [32,33]. Normality of $\log_{10}$ EC_{50} was checked with the Shapiro–Wilk test.

Fungicides were compared on the same isolates with the Friedman test and with pairwise Wilcoxon signed-rank tests on $\log_{10}$ EC_{50}, adjusted by Holm's method [34]. Cross-sensitivity was assessed with Spearman correlations among $\log_{10}$ EC_{50} values and copper inhibition at 100 μg mL^{-1}. Effects of canton, cacao genotype and farm were tested with the Kruskal–Wallis test. Each farm grew mainly one cacao genotype, so cacao genotype and farm are confounded in this collection, and every test involving cacao genotype is read as descriptive. To test whether isolates from one field sample were alike, the mean absolute difference in $\log_{10}$ EC_{50} within the seven same-sample pairs was compared with its distribution over 5000 random pairings of the 23 isolates.

The azoxystrobin values appeared to fall into two groups, so a two-component normal mixture was fitted to $\log_{10}$ EC_{50} (censored values entered as 0.005 μg mL^{-1}) with the expectation–maximization algorithm of mixtools [35]. It was compared with a single normal distribution by the likelihood ratio (LR). The null distribution of the LR came from a parametric bootstrap of 500 data sets simulated under the single normal [36], and the Bayesian information criterion (BIC) was compared as well. Each isolate was assigned to the component with the higher posterior probability. Association of the resulting phenotypes with farm, canton and cacao genotype was tested with chi-square tests whose *p*-values were obtained by Monte Carlo simulation (20,000 replicates).

To summarize joint sensitivity, the $\log_{10}$ EC_{50} values of difenoconazole, boscalid and azoxystrobin were standardized to *z*-scores and clustered with Euclidean distance and Ward's linkage [37]. Copper had no effect and was left out of the clustering; its inhibition at 100 μg mL^{-1} is shown only as an annotation. Clustering quality was assessed with the cophenetic correlation and the mean silhouette width for two to six groups [38]. The number of groups chosen was the one with the highest silhouette among partitions in which every group held at least two isolates. Cluster stability was

© 2026 by the author(s). Distributed under a Creative Commons CC BY license.

Preprints.org | NOT PEER-REVIEWED | Posted: 17 November 2026 https://doi.org/10.20944/preprints202611.1684.v1

measured as the mean Jaccard similarity over 1000 bootstrap resamples of isolates [39], and the association of clusters with origin was tested as above (Monte Carlo chi-square, 20,000 replicates).

2.7. Principal Component Analysis

A principal component analysis (PCA) [40] was run on 12 variables, the relative AUMGC of each isolate at 0.1, 1 and 10 µg mL^{-1} of each of the four fungicides, where responses differed most among isolates. The variables were centred and scaled to unit variance. Two missing values were replaced by the mean of the corresponding fungicide and concentration. Scores on the first two components were compared between azoxystrobin phenotypes with the Wilcoxon rank-sum test and among farms, cantons and cacao genotypes with the Kruskal–Wallis test. The full standardized profile was also tested by permutational multivariate analysis of variance (PERMANOVA) on Euclidean distances [41], with 9999 permutations, separately for azoxystrobin phenotype, farm, canton and cacao genotype. A complementary PCA was run on the standardized $\log_{10}$ EC_{50} values of difenoconazole, boscalid and azoxystrobin.

2.8. Simulation of 300 Additional Isolates

For each fungicide, 300 additional isolates were simulated by two methods, each with 10,000 replicates. In the parametric Monte Carlo method (M1), each replicate drew the mean and standard deviation of $\log_{10}$ EC_{50} from the 1000 cluster-bootstrap estimates, which carried parameter uncertainty forward, and then drew 300 log-normal values. For azoxystrobin, each replicate instead drew a set of mixture parameters re-estimated in 500 cluster-bootstrap resamples. In the cluster smoothed bootstrap (M2), each simulated isolate was obtained by resampling a field sample, then one isolate within it, and adding Gaussian noise on the $\log_{10}$ scale. The bandwidth followed Silverman's rule [42] and was 0.14 for difenoconazole, 0.081 for boscalid and 0.41 for azoxystrobin. Each replicate gave category counts, the median and the P95. For azoxystrobin, the number of isolates with $EC_{50} \geq 0.3$ µg mL^{-1} (the gap between the two observed phenotypes) was also recorded. Results are given with 95% prediction intervals (PI), the 2.5th and 97.5th percentiles across replicates. Agreement between methods was measured with the Kolmogorov–Smirnov distance (D). The simulated isolates are model predictions, used only to express uncertainty and plan sampling.

2.9. Precision and Power for Monitoring Design

From the fitted log-normal parameters, 3000 samples of n isolates (n = 10 to 323) were simulated. In each, the median was estimated as the sample mean of $\log_{10}$ EC_{50} and the P95 as that mean plus 1.645 standard deviations. Precision was expressed as a fold half-width, 10 raised to half the distance between the 2.5th and 97.5th percentiles of the estimates on the $\log_{10}$ scale. A value of 1.5 means that the quantity is known within a factor of 1.5. The power of a two-sided t-test on $\log_{10}$ EC_{50} (α = 0.05) was computed from the noncentral t distribution for a 2-, 3-, 5- or 10-fold increase in the median. Baselines of 23, 123 or 323 isolates (the present collection alone or enlarged by 100 or 300) were compared with later samples of 23, 50, 100 or 300 isolates. For azoxystrobin these calculations assume a single log-normal distribution and therefore understate the true uncertainty.

2.10. Software

All analyses were run in R 4.3.3 [43] with the random seed 20261025. Dose–response models were fitted with drc [25] and checked with ec50estimator [27]. AUMGC and Tukey's tests were computed with agricolae [44] (audpc, HSD.test), censored fits with survreg from survival [31], and the mixture model with normalmixEM and boot.comp from mixtools [35]. Silhouette widths came from the cluster package and cluster stability from clusterboot in fpc [39]. Figures were drawn with ggplot2 [45], ggrepel and gridExtra. The remaining tests, hierarchical clustering and PCA (prcomp) used base R functions.

© 2026 by the author(s). Distributed under a Creative Commons CC BY license.

Preprints.org | NOT PEER-REVIEWED | Posted: 17 November 2026 https://doi.org/10.20944/preprints202611.1684.v1

3. Results

3.1. Growth and Area Under the Growth Curve

Control colonies grew almost linearly between 48 and 120 h and reached a mean growth of 20.7–24.8 mm at 120 h, depending on the assay (Figure 1). Isolates differed in vigour in all four assays (Kruskal–Wallis on control AUMGC, $p < 0.0001$), which will matter later for boscalid. Each fungicide produced its own pattern (Figure 2). Difenoconazole cut relative AUMGC to 66.0% at 0.1 µg mL^{-1} and to 19.1% at 1 µg mL^{-1}, and nothing grew at 100 µg mL^{-1} ($F_{5,105} = 461.5$, $p < 0.001$). Boscalid did nothing up to 0.1 µg mL^{-1} and then acted steeply, from 42.4% at 1 µg mL^{-1} to 4.7% at 10 µg mL^{-1} ($F_{5,105} = 477.6$, $p < 0.001$). Azoxystrobin slowed growth from the lowest concentration but never stopped it. At 100 µg mL^{-1} relative AUMGC was still 18.4% ($F_{5,110} = 96.4$, $p < 0.001$), and the means at 10 and 100 µg mL^{-1} did not differ (Tukey groups de and e). Copper sulfate had no effect at any concentration (95.6–102.9%; $F_{5,110} = 0.55$, $p = 0.74$).

At 0.01 µg mL^{-1} the four fungicides were alike ($p = 0.082$; Friedman $p = 0.094$). From 0.1 µg mL^{-1} upwards they were not (Friedman $p < 0.001$ at every concentration), and their ranking changed with dose. At 0.1 µg mL^{-1} azoxystrobin (69.6%) matched difenoconazole (67.5%), while boscalid and copper had not yet acted. At 10 and 100 µg mL^{-1} azoxystrobin fell behind both difenoconazole and boscalid, which had stopped growth (Table S4). Copper sulfate was the least active at every concentration. Within isolates, concentration affected AUMGC in all 23 isolates for azoxystrobin and in 22 each for boscalid and difenoconazole. It also did so in 13 isolates for copper sulfate, but erratically and with no dose–response pattern (Table S2; Figures S1–S4). Canton had no effect on relative AUMGC ($p = 0.24$–0.47). Cacao genotype showed a marginal association for difenoconazole only ($p = 0.047$), with median relative AUMGC of 34.1% for isolates from CCN51, 39.7% from Súper Árbol and 44.9% from Nacional trees. Since cacao genotype and farm are confounded, this describes the collection rather than a host effect.

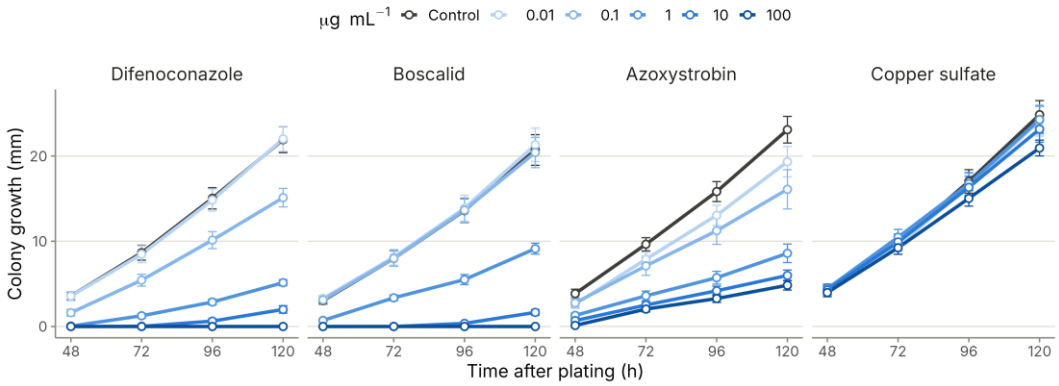


Figure 1. Colony growth of 23 *Moniliophthora roreri* isolates from 48 to 120 h on PDA amended with difenoconazole, boscalid, azoxystrobin or copper sulfate. Growth is the mean of two perpendicular colony diameters minus the diameter of the mycelial disc. Points are means over isolates and bars standard errors. The dark grey line is the control, and blue lines darken with concentration (µg mL^{-1}).

© 2026 by the author(s). Distributed under a Creative Commons CC BY license.

Preprints.org | NOT PEER-REVIEWED | Posted: 17 November 2026 https://doi.org/10.20944/preprints202611.1684.v1

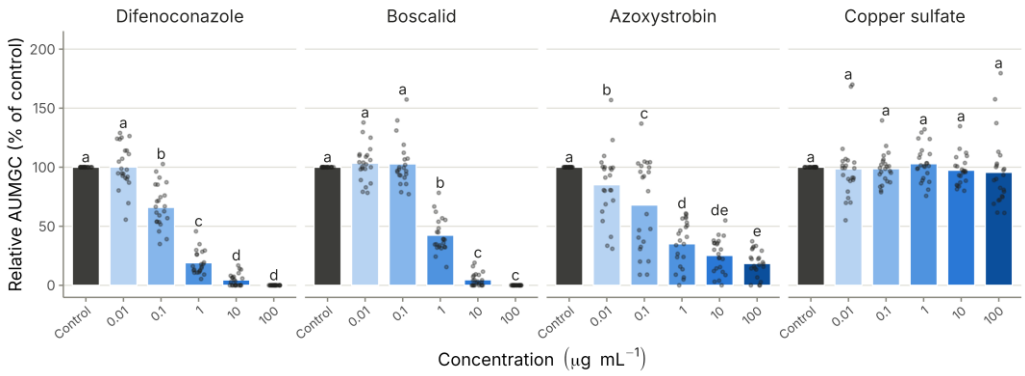


Figure 2. Relative area under the mycelial growth curve (AUMGC, % of the control of the same isolate) of 23 *M. roreri* isolates at each fungicide concentration. Bars are means and grey points individual isolates. Within each panel, bars with different letters differ significantly (randomized complete block ANOVA with isolates as blocks, Tukey's HSD, $\alpha = 0.05$).

3.2. EC_{50} Distributions

Difenoconazole was the most active fungicide (Table 3; Figure 3). Its EC_{50} values ran from 0.103 μg mL^{-1} (C14) to 1.17 μg mL^{-1} (C17), an 11.4-fold span, and were log-normally distributed (Shapiro–Wilk on $\log_{10}$ values, $p = 0.41$). Only C17 left the highly sensitive category. Boscalid was about three times less active (median ratio of paired values 0.33; Wilcoxon, $p_{Holm} < 0.001$). Its distribution was narrow except for an upper tail of three isolates, C15 (2.27 μg mL^{-1}), C22 (3.26 μg mL^{-1}) and C23 (6.76 μg mL^{-1}, the only moderately sensitive isolate). That tail needs confirmation. C20, C22 and C23 grew very slowly on their boscalid control plates (MGR 1.7, 1.5 and 1.2 mm day^{-1}, against 3.2–9.7 mm day^{-1} in the other isolates), so their boscalid EC_{50} values rest on small absolute differences in growth. Without them the geometric mean was 0.89 μg mL^{-1}, the maximum 2.27 μg mL^{-1}, and the distribution was log-normal ($p = 0.24$).

Copper sulfate never reached 50% inhibition, so all 23 EC_{50} values lie above the tested range. Mean inhibition at that concentration was 11.0% (range −55.2 to 37.4%), and six isolates exceeded 30%. Three of them went the other way. C4, C6 and C7 grew more on copper than on their controls.

Azoxystrobin spanned about 200-fold, from 0.0071 μg mL^{-1} (C5) to 1.43 μg mL^{-1} (C8), and two isolates, C5 and C11, fell below the lowest concentration tested. In paired comparisons azoxystrobin did not differ from difenoconazole ($p = 0.20$), and boscalid values exceeded azoxystrobin values by a median factor of 3.75 ($p_{Holm} = 0.002$; Friedman $\chi^2 = 15.2$, $p < 0.001$ across the three fungicides). A single log-normal distribution fitted azoxystrobin badly (Shapiro–Wilk $p = 0.001$), so its GM, GSD and upper percentiles in Table 3 need to be read with Section 3.3 in mind. Residual growth at the lower asymptote of the azoxystrobin curves ranged from 0 to 43% of the control, with a median of 26%. EC_{50} values from the 120-h diameter were close to those from MGR (median ratios 0.79–1.02).

Sensitivities to the three single-site fungicides were largely independent of one another. Azoxystrobin and difenoconazole were the only correlated pair (Spearman $\varrho = 0.46$, $p = 0.029$). Azoxystrobin and boscalid ($\varrho = 0.17$, $p = 0.45$) and boscalid and difenoconazole ($\varrho = -0.03$, $p = 0.91$) were not, and copper inhibition was unrelated to any of them ($|\varrho| \leq 0.21$, $p \geq 0.34$). Canton, cacao genotype and farm had no detectable effect on the EC_{50} of difenoconazole ($p = 0.13$, 0.33 and 0.19) or boscalid ($p = 0.97$, 0.80 and 0.36). For azoxystrobin, geometric means ranged from 0.022 μg mL^{-1} at La Calumeña to 0.85 μg mL^{-1} at La Belleza, yet the rank test on farm only approached significance ($p = 0.057$; canton $p = 0.59$, cacao genotype $p = 0.10$).

© 2026 by the author(s). Distributed under a Creative Commons CC BY license.

Preprints.org | NOT PEER-REVIEWED | Posted: 17 November 2026 https://doi.org/10.20944/preprints202611.1684.v1

Table 3. EC_{50} (μg mL^{-1}) of difenoconazole, boscalid, azoxystrobin and copper sulfate for 23 *Moniliophthora roreri* isolates.

Fungicide	Range	GM [95% CI]	GSD	P95 [95% CI]	P99 [95% CI]	HS/S/MS/LS/VLS
Difenoconazole	0.103–1.17	0.323 [0.242–0.438]	1.96	0.98 [0.62–1.36]	1.54 [0.89–2.29]	22/1/0/0/0
Boscalid	0.535–6.76	1.02 [0.79–1.37]	1.80	2.70 [1.26–4.99]	4.04 [1.51–8.90]	15/7/1/0/0
without C20, C22, C23 [a]	0.535–2.27	0.89	—	—	—	14/6/0/0/0
Azoxystrobin, all [b]	<0.01–1.43	0.185 [0.062–0.441]	7.15	4.71 [1.77–8.13]	18.0 [6.0–37.4]	18/5/0/0/0
sensitive (n = 11)	<0.01–0.217 [c]	0.035	—	—	—	11/0/0/0/0
less sensitive (n = 12)	0.695–1.43	1.00	—	—	—	7/5/0/0/0
Copper sulfate	>100 (all)	—	—	—	—	0/0/0/0/23

GM, geometric mean (median of the fitted log-normal distribution); GSD, geometric standard deviation; P95 and P99, 95th and 99th percentiles. CIs from a cluster bootstrap over the 16 field samples (1000 replicates). HS, highly sensitive (<1 μg mL^{-1}); S, sensitive (1–5); MS, moderately sensitive (>5–20); LS, low sensitivity (>20–100); VLS, very low sensitivity (>100); values are numbers of isolates. [a] Isolates with low-vigour control plates (Section 3.2). [b] Single log-normal fit, inadequate for a bimodal distribution (Section 3.3); the fitted P95 and P99 lie above the highest observed value. [c] Includes two isolates with model estimates below the lowest concentration tested (0.0071 and 0.0087 μg mL^{-1}). Per-isolate values with bootstrap and delta-method confidence intervals are given in Table S1.

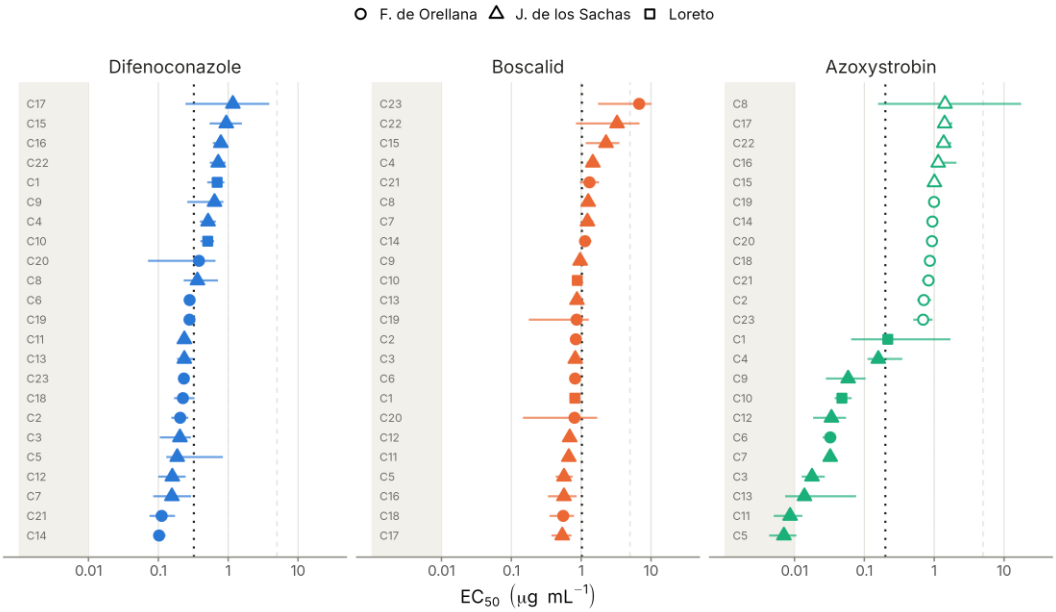


Figure 3. EC_{50} of difenoconazole, boscalid and azoxystrobin for 23 *M. roreri* isolates, ordered by value. Symbols are point estimates and horizontal lines 95% bootstrap percentile intervals (300 resamples of plates within concentrations). Symbol shape indicates canton; for azoxystrobin, open symbols mark the less sensitive phenotype. The dotted line is the geometric mean of the estimates, the dashed line marks the category limit at 5 μg mL^{-1}, and the shaded area lies below the lowest concentration tested (0.01 μg mL^{-1}). Copper sulfate is not shown because all isolates had EC_{50} > 100 μg mL^{-1}.

© 2026 by the author(s). Distributed under a Creative Commons CC BY license.

Preprints.org | NOT PEER-REVIEWED | Posted: 17 November 2026 https://doi.org/10.20944/preprints202611.1684.v1

3.3. Two Azoxystrobin Phenotypes

The azoxystrobin values fell into two clusters with an empty stretch between them (Figure 4A). A two-component mixture fitted far better than one log-normal distribution (LR = 29.8; parametric bootstrap $p = 0.002$; BIC 42.9 vs. 63.3). Eleven isolates (C1, C3, C4, C5, C6, C7, C9, C10, C11, C12 and C13) formed a sensitive group, with EC_{50} values from below 0.01 to 0.217 µg mL^{-1} (GM 0.035 µg mL^{-1}). The other 12 (C2, C8 and C14–C23) formed a less sensitive group from 0.695 to 1.43 µg mL^{-1} (GM 1.00 µg mL^{-1}). No isolate fell between 0.22 and 0.69 µg mL^{-1}. The observed group means were about 30-fold apart, and the mixture components 32-fold (0.031 vs. 1.00 µg mL^{-1}), with a weight of 0.48 for the sensitive one.

The dose–response curves show what the split means on a plate (Figure 4B). At 0.01 and 0.1 µg mL^{-1} the less sensitive isolates were not inhibited at all (mean inhibition of MGR −5.8% and 1.4%). The sensitive ones had already lost 30.4% and 66.7% of their growth rate. The less sensitive group reached 48.8% inhibition at 1 µg mL^{-1} and 69.8% at 100 µg mL^{-1}. All azoxystrobin plates were sown on the same day, which rules out a batch effect.

Where the isolates came from mattered. The less sensitive phenotype accounted for all seven isolates from La Belleza, four of the five from San Carlos and one of three from Unión Milagreña (C22). None of the eight isolates from La Calumeña, La Paz and Bajo Huiruno had it (farm, Monte Carlo $p < 0.001$). Seven of the eight Francisco de Orellana isolates were less sensitive (canton, $p = 0.025$). The exception, C6, came from Bajo Huiruno, a community that field records place in Loreto [9]. Sorted by the cacao genotype of the host tree, the less sensitive isolates were seven of nine from CCN51, four of six from Nacional and one of eight from Súper Árbol ($p = 0.026$). This association is descriptive. Cacao genotype and farm are confounded in this collection, because each farm grew mainly one cacao genotype, and farm is the better-supported factor. Isolates from the same field sample were much more alike than random pairs (mean absolute difference in $\log_{10}$ EC_{50} 0.24 vs. 0.90; $p = 0.001$). Six of the seven pairs fell in the same phenotype. The odd pair was C4 (sensitive) and C22 (less sensitive). For difenoconazole and boscalid the same comparison gave weaker trends that did not reach significance (0.22 vs. 0.34, $p = 0.078$; 0.16 vs. 0.27, $p = 0.068$).

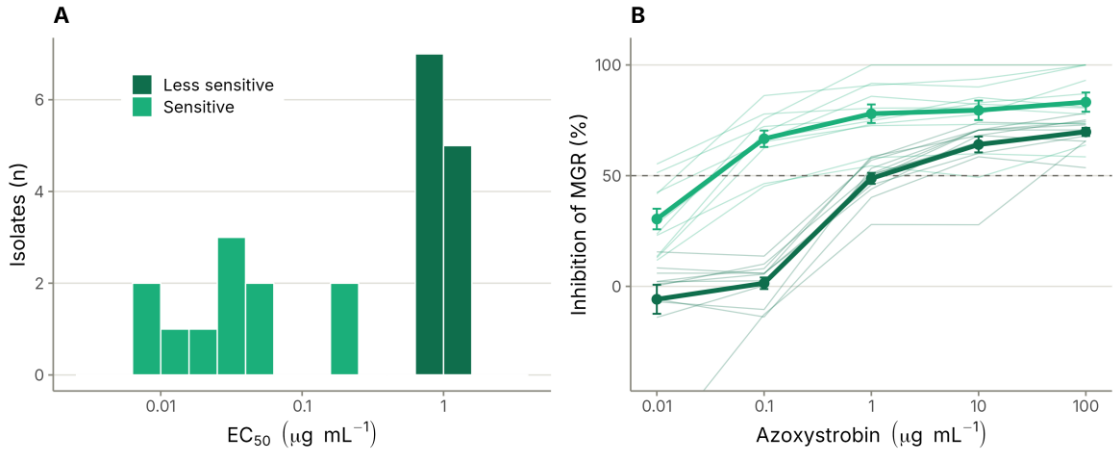


Figure 4. Two azoxystrobin phenotypes among 23 *M. roreri* isolates. (**A**) Distribution of EC_{50} values on a logarithmic scale, coloured by the phenotype assigned by the two-component mixture model. (**B**) Inhibition of the mycelial growth rate (MGR) relative to the control. Thin lines are individual isolates and thick lines group means ± standard error; the dashed line marks 50% inhibition.

3.4. Joint Sensitivity Profiles

Ward clustering of the standardized EC_{50} values gave five groups (Figure 5). The mean silhouette width rose from 0.32 for two groups to 0.46 for five. Six groups scored 0.48 but left an isolate on its own. The cophenetic correlation was 0.66, a moderate fit. The first split of the tree separated seven of the 11 azoxystrobin-sensitive isolates (G1: C3, C5, C6, C7, C11, C12 and C13; azoxystrobin GM 0.018

© 2026 by the author(s). Distributed under a Creative Commons CC BY license.

Preprints.org | NOT PEER-REVIEWED | Posted: 17 November 2026 https://doi.org/10.20944/preprints202611.1684.v1

μg mL⁻¹) from everything else. G1 was also the most stable group (Jaccard 0.98). The other four sensitive isolates formed G5 (C1, C4, C9 and C10; Jaccard 0.79), with intermediate azoxystrobin values (GM 0.099 μg mL⁻¹) and fairly high difenoconazole values (0.58 μg mL⁻¹).

The less sensitive isolates fell into three groups. G3 (C2, C8, C14, C18, C19, C20 and C21; Jaccard 0.86) held six La Belleza isolates plus C8 from San Carlos. G2 (C15, C22 and C23; Jaccard 0.78) had the highest boscalid values (GM 3.68 μg mL⁻¹), but two of its three members are the low-vigour isolates C22 and C23. G4 (C16 and C17) was the least stable group (Jaccard 0.66). It joined two Nacional isolates from San Carlos with the highest difenoconazole values (GM 0.96 μg mL⁻¹). Azoxystrobin separated the groups most strongly (Kruskal–Wallis $p < 0.001$), then difenoconazole ($p = 0.008$) and boscalid ($p = 0.014$). Copper inhibition did not differ among them ($p = 0.79$). Cluster membership was associated with farm (Monte Carlo $p = 0.003$), canton ($p = 0.006$) and cacao genotype ($p = 0.014$). The last association is descriptive, because each farm grew mainly one cacao genotype.

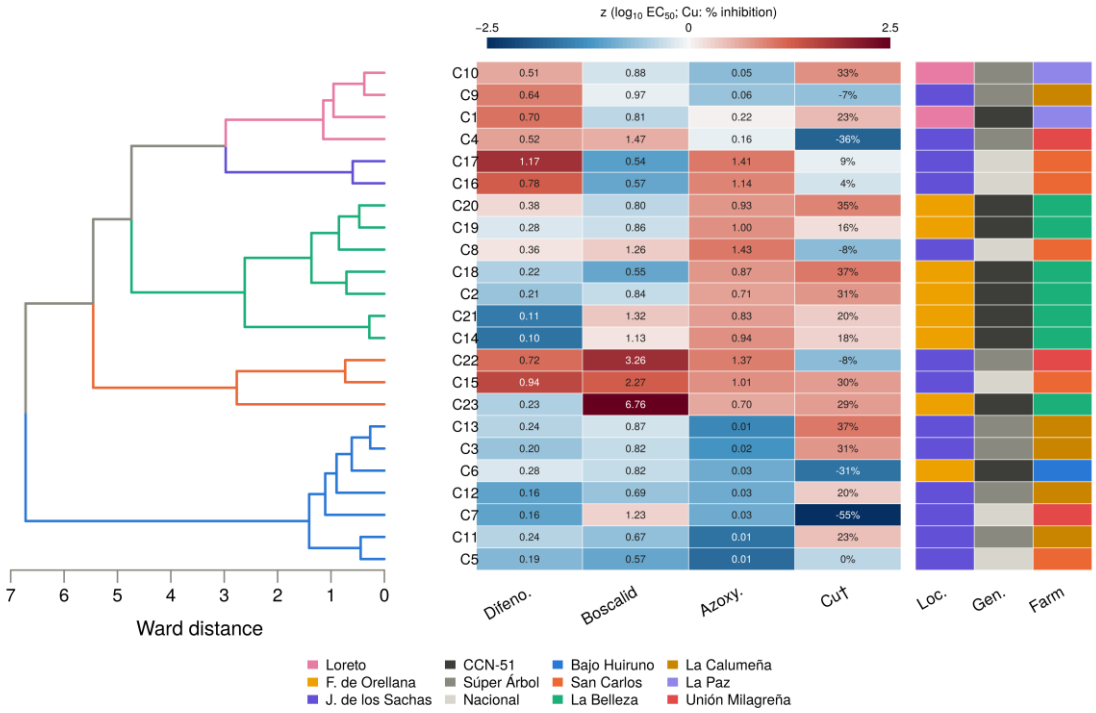


Figure 5. Ward clustering of 23 *M. roreri* isolates by the standardized $\log_{10}$ EC_{50} of difenoconazole (Difeno.), boscalid and azoxystrobin (Azoxy.). Branch colours identify the five groups (blue, G1; orange, G2; green, G3; purple, G4; pink, G5). Cell colours are *z*-scores, and the numbers in the cells are EC_{50} values (μg mL⁻¹). The copper column (Cu†) shows percentage inhibition at 100 μg mL⁻¹ and was not used for clustering. Side bars indicate canton (Loc.), cacao genotype (Gen.) and farm.

3.5. Principal Components of the Growth Profiles

Would the azoxystrobin split show up without telling the analysis which isolate belonged where? It did. The first three components took 35.1%, 19.5% and 15.3% of the variance (69.9% together). PC1 was the azoxystrobin axis. The three azoxystrobin variables loaded on it at 0.39–0.42, difenoconazole at 1 and 10 μg mL⁻¹ at 0.27–0.36 and boscalid at 0.18–0.24, while the copper variables loaded negatively (−0.16 to −0.27; Figure 6B). A high PC1 score means comparatively good growth on the fungicides, above all on azoxystrobin. The two phenotypes separated along PC1 (Wilcoxon $p < 0.001$) and overlapped on PC2 ($p = 0.31$; Figure 6A). C7, C12, C13 and C11, four of the most azoxystrobin-sensitive isolates, sat at the negative end. C15 and C22, which also had high boscalid values, and the San Carlos pair C16 and C17 sat at the positive end.

© 2026 by the author(s). Distributed under a Creative Commons CC BY license.

Preprints.org | NOT PEER-REVIEWED | Posted: 17 November 2026 https://doi.org/10.20944/preprints202611.1684.v1

PC2 was copper. Its loadings came from the copper variables (0.47–0.52) and from boscalid at 10 µg mL^{-1} (0.37), and it ordered isolates by their erratic response to copper sulfate. We read it as noise.

PERMANOVA on the whole 12-variable profile told the same story. Azoxystrobin phenotype explained 23% of the multivariate variation (pseudo-F = 6.14, R^2 = 0.23, p < 0.001) and farm 35% (F = 1.84, R^2 = 0.35, p = 0.018). Cacao genotype (R^2 = 0.14, p = 0.076) and canton (R^2 = 0.10, p = 0.38) did not reach significance. Farm has five degrees of freedom against one for phenotype, which inflates its R^2 and lowers its F. On PC1 alone, farm came close (Kruskal–Wallis p = 0.052), while canton (p = 0.90) and cacao genotype (p = 0.17) did not.

The complementary PCA on $\log_{10}$ EC_{50} produced a first component (48.8%) on which all three fungicides loaded with the same sign (azoxystrobin −0.69, boscalid −0.52, difenoconazole −0.51), a general sensitivity axis. The second component (31.8%) set difenoconazole (0.72) against boscalid (−0.70). We found no sign of cross-sensitivity between them.

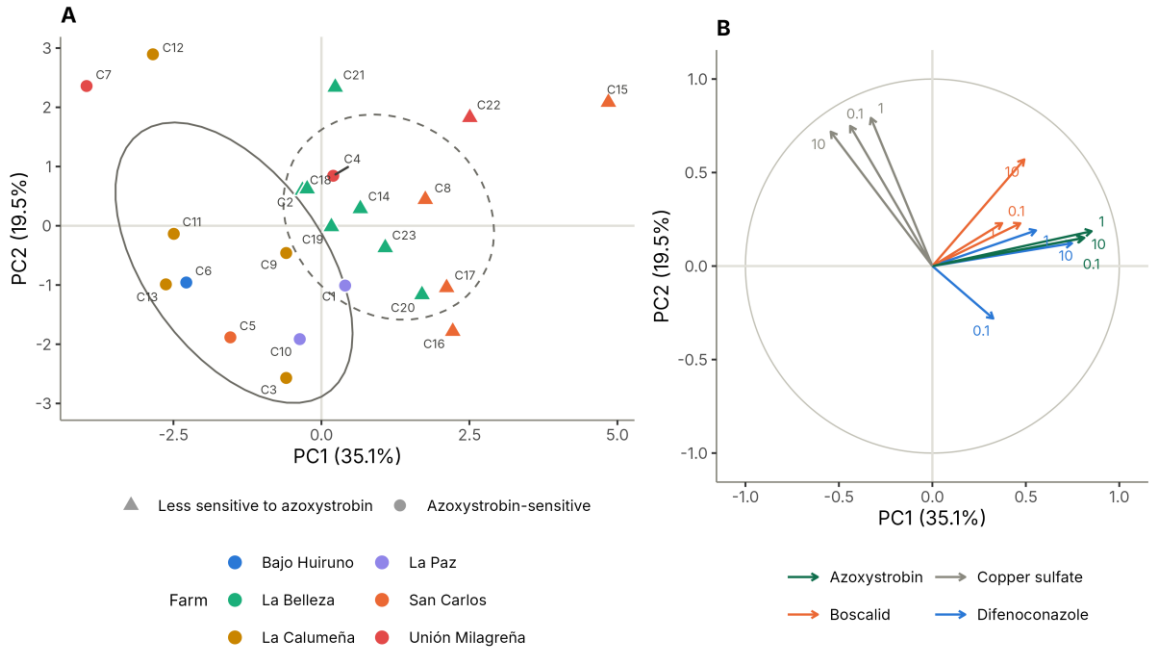


Figure 6. Principal component analysis of the relative AUMGC of 23 *M. roreri* isolates at 0.1, 1 and 10 µg mL^{-1} of difenoconazole, boscalid, azoxystrobin and copper sulfate (12 standardized variables). (**A**) Isolate scores on PC1 and PC2. Colour indicates farm and symbol shape the azoxystrobin phenotype (circles, sensitive; triangles, less sensitive). Ellipses enclose 68% of a bivariate normal distribution fitted to each phenotype (solid, sensitive; dashed, less sensitive). (**B**) Correlation circle. Arrows show the correlation of each variable with PC1 and PC2, coloured by fungicide and labelled with the concentration (µg mL^{-1}).

3.6. What 300 More Isolates Might Look Like

Both simulation methods predicted that about nine in ten new isolates would be highly sensitive to difenoconazole (273.5 and 286.1 of 300, on average) and that practically none would exceed 5 µg mL^{-1} (Table 4; Figure 7). For boscalid they disagreed. M1 predicted roughly equal numbers of highly sensitive and sensitive isolates. M2, which resamples the tail formed by C22 and C23, predicted about 18 moderately sensitive isolates per 300, against about two with M1.

For azoxystrobin, both methods put about three-quarters of the isolates in the highly sensitive category and nearly all the rest in the sensitive one. Those categories hide the real uncertainty, which is the mix of phenotypes. M1 predicted 158.9 less sensitive isolates of 300 (53%; 95% PI 85–227) and M2 predicted 136.0 (45%; 119–153). Fewer than 0.2 of every 300 simulated isolates, on average, exceeded 20 µg mL^{-1} for any fungicide.

© 2026 by the author(s). Distributed under a Creative Commons CC BY license.

Preprints.org | NOT PEER-REVIEWED | Posted: 17 November 2026 https://doi.org/10.20944/preprints202611.1684.v1

The two methods agreed at the centre of the distributions and parted in the tails (KS D = 0.084 for difenoconazole, 0.135 for boscalid and 0.156 for azoxystrobin). M2 placed 51.3 of every 300 simulated isolates above the highest observed EC_{50}, against 13.4 with M1, and its azoxystrobin P95 was higher accordingly (3.35 vs. 1.37 μg mL^{-1}). The simulated azoxystrobin median also depended on the method (0.63 vs. 0.21 μg mL^{-1}). It falls in the gap between the phenotypes and tracks the proportion of each.

Table 4. Expected number of isolates in each sensitivity category, median and P95 among 300 simulated *Moniliophthora roreri* isolates over 10,000 replicates. Counts are means and the median and P95 are medians across replicates, each with its 95% prediction interval. The simulated isolates are model predictions, not observations.

Fungicide	Method	HS (<1)	S (1–5)	MS (>5–20)	Median (μg mL^{-1})	P95 (μg mL^{-1})	Less sensitive (of 300)
Difenoconazole	M1	286.1 [264–299]	13.8 [1–36]	≈0	0.32 [0.24–0.44]	0.94 [0.60–1.41]	—
	M2	273.5 [263–283]	26.5 [17–37]	≈0	0.31 [0.27–0.35]	1.18 [1.03–1.35]	—
Boscalid	M1	150.9 [97–239]	146.6 [61–196]	2.5 [0–15]	1.02 [0.79–1.38]	2.60 [1.25–5.01]	—
	M2	189.3 [173–205]	92.8 [77–108]	17.9 [10–26]	0.86 [0.82–0.92]	5.66 [3.22–6.80]	—
Azoxystrobin	M1	223.9 [168–273]	75.4 [24–132]	0.6 [0–9]	0.63 [0.04–0.94]	1.37 [1.08–3.69]	158.9 [85–227] (53%)
	M2	228.0 [213–242]	64.9 [51–79]	7.0 [2–12]	0.21 [0.12–0.33]	3.35 [2.56–4.42]	136.0 [119–153] (45%)

M1, parametric Monte Carlo (log-normal distribution for difenoconazole and boscalid; two-component mixture for azoxystrobin; parameters drawn from cluster-bootstrap estimates); M2, cluster smoothed bootstrap (resampling of field samples and isolates with Gaussian kernel noise). HS, highly sensitive; S, sensitive; MS, moderately sensitive (EC_{50} classes in μg mL^{-1}). Isolates with EC_{50} > 20 μg mL^{-1} were practically absent (mean ≤0.16 per 300 in every scenario). Less sensitive, number of simulated azoxystrobin isolates with EC_{50} ≥ 0.3 μg mL^{-1}, with the percentage of 300 in parentheses. Copper sulfate was not simulated because no EC_{50} value lay within the tested range.

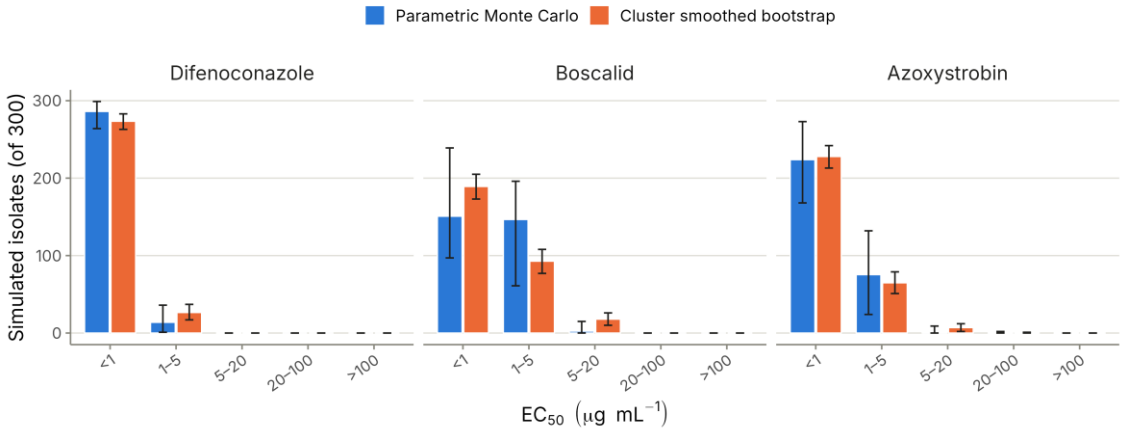


Figure 7. Expected number of isolates per EC_{50} category among 300 simulated *M. roreri* isolates, by parametric Monte Carlo (M1, blue) and cluster smoothed bootstrap (M2, orange). Bars are means and whiskers 95% prediction intervals over 10,000 replicates. Simulated isolates are model predictions, not observations.

© 2026 by the author(s). Distributed under a Creative Commons CC BY license.

Preprints.org | NOT PEER-REVIEWED | Posted: 17 November 2026 https://doi.org/10.20944/preprints202611.1684.v1

3.7. Monitoring Design and Candidate Discriminatory Concentrations

Precision improved fast up to about 50 isolates and slowly after that (Figure 8A). With the present 23 isolates the P95 is known within a factor of 1.54 for difenoconazole and 1.45 for boscalid. For azoxystrobin the factor is 3.41. Adding 100 isolates would bring these to 1.20, 1.18 and 1.71, and adding 300 to 1.12, 1.10 and 1.39. The median is known more tightly (1.32, 1.27 and 2.27 with 23 isolates).

Power followed the same order. Two sets of 23 isolates would detect a twofold shift in the median EC_{50} with a power of 0.93 for difenoconazole and 0.97 for boscalid. For azoxystrobin the same comparison had a power of 0.22 for a twofold shift and 0.46 for a threefold one. Enlarging only the later sample helped little (0.37 and 0.73 with 23 vs. 300 isolates). Enlarging the baseline helped a lot. With 123 baseline isolates and a later sample of 100, power rose to 0.74 and 0.99, and with 323 baseline isolates to 0.87 and 1.00 (Figure 8B).

The data also point to provisional discriminatory concentrations. For difenoconazole, 1 μg mL^{-1} inhibited MGR by more than 50% in 21 of 23 isolates. C15 fell just short (49%), and C5 had no reading at that concentration. That concentration sits just above the P95 (0.98 μg mL^{-1}) and below the upper confidence limit of the P99 (2.29 μg mL^{-1}). For boscalid, 5 μg mL^{-1} lies above the P95 (2.70 μg mL^{-1}). Ten μg mL^{-1} is too close to the plateau. It cut relative AUMGC to 4.7% on average but inhibited MGR by more than 90% in only 13 of 23 isolates. For azoxystrobin, 0.1 μg mL^{-1} separated the two phenotypes cleanly. Mean inhibition of MGR was 66.7% (range 45.2–86.2%) in the sensitive isolates and 1.4% (−13.8 to 13.7%) in the less sensitive ones.

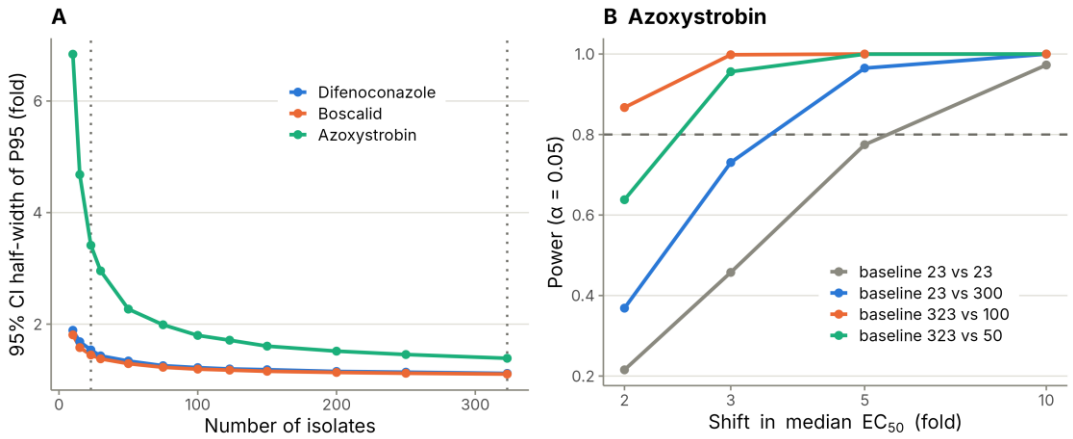


Figure 8. (**A**) Fold half-width of the 95% interval of the estimated P95 of EC_{50} as a function of the number of isolates (3000 simulated samples per size, single log-normal distribution). Dotted lines mark the present collection (n = 23) and the collection enlarged by 300 isolates (n = 323). (**B**) Power of a two-sided t-test on $\log_{10}$ EC_{50} (α = 0.05) to detect an increase in the median EC_{50} of azoxystrobin, for four combinations of baseline and later sample sizes (23 vs. 23, 23 vs. 300, 323 vs. 100 and 323 vs. 50 isolates). The dashed line marks a power of 0.8.

4. Discussion

Difenoconazole and boscalid inhibited every *M. roreri* isolate from Orellana within a narrow band of low concentrations. Copper sulfate did nothing measurable to mycelial growth. Azoxystrobin was the odd one. It split the collection into two phenotypes about 30-fold apart, and the split followed the farm of origin. It is the result that matters most for disease management and the least settled.

4.1. Two Azoxystrobin Phenotypes: A Shift Hypothesis

Isolates that have never met a fungicide usually vary continuously, around a single mode. A discrete step, with an empty gap between two groups, is what one expects when part of the population carries a mechanism of large effect [16–18]. QoIs are the textbook case. FRAC puts them in its

© 2026 by the author(s). Distributed under a Creative Commons CC BY license.

Preprints.org | NOT PEER-REVIEWED | Posted: 17 November 2026 https://doi.org/10.20944/preprints202611.1684.v1

high-risk group, and resistance appeared in several pathogens within a few years of their release [15,46,47]. The size of the step hints at the mechanism. The G143A substitution in cytochrome *b* typically raises EC_{50} more than 100-fold and leads to loss of field control, whereas F129L and G137R give partial resistance with moderate shifts [47–49]. A 30-fold step looks more like the second kind. In rusts, *A. solani* and *Pyrenophora teres* an intron right after codon 143 makes G143A impair splicing, and resistance has been limited to F129L [49,50]. The *cytb* gene of *M. perniciosa* carries two introns [51], and the mitochondrial genome of *M. roreri* has been sequenced [52]. As far as we know, nobody has checked where those introns lie relative to codon 143.

Alternative respiration offers a second explanation, and the two are not exclusive. The alternative oxidase lets mycelium bypass a blocked cytochrome bc_1 complex, and it is a well-known reason why QoIs look weaker in vitro than in planta [26]. In the closely related *M. perniciosa* the alternative oxidase is needed for biotrophic development, and growth in vitro responds to inhibitors of both respiratory pathways [53]. Both phenotypes kept some growth at high azoxystrobin concentrations (Figure 4B), so we suspect every isolate has some alternative respiration. Whether the less sensitive ones lean on it more is an open question. Our assays measured mycelial growth without salicylhydroxamic acid (SHAM), which blocks the alternative pathway and is often used in QoI baselines [26,54], and *cytb* has not yet been sequenced. The less sensitive phenotype therefore stands as a hypothesis of a shift; resistance has not been demonstrated. The isolates are preserved, so the hypothesis can be tested directly. The next step is to assay both phenotypes with SHAM and by spore germination, and to sequence codons 129, 137 and 143 of *cytb*.

Where the less sensitive isolates came from fits the shift hypothesis without proving it. They dominated La Belleza, a commercial CCN51 farm, and San Carlos, a Nacional farm. They were absent from the Súper Árbol farm La Calumeña and from the two farms of Puerto Murialdo. Each farm grew mainly one cacao genotype, so cacao genotype and farm are confounded in this collection, and the association with cacao genotype reported above is descriptive. It tells us which trees the isolates came from, not that the host shapes the sensitivity of its pathogen. Farm is the better-supported factor, and spray history, which varies from farm to farm, offers a direct route to selection. No application records exist for these farms, so recording spray history from now on is the obvious next step (Section 4.5). The PCA, which knew nothing of the groups, put azoxystrobin on its main axis, and PERMANOVA gave farm a significant share of the profile while cacao genotype and canton fell short. We did not expect a rank test on farm to miss significance ($p = 0.057$) when the categorical test was so clear ($p < 0.001$). The explanation is mundane. With one to seven isolates per farm and a trait that is essentially two-valued, ranks waste most of the information.

Espinoza-Lozano et al. [19] found 76 Ecuadorian isolates, Amazonian ones among them, to be highly sensitive to azoxystrobin, with IC_{50} values mostly below 0.015 μg mL^{-1}. Our sensitive group (GM 0.035 μg mL^{-1}) lies in the same order of magnitude. Our less sensitive group lies about two orders above it. Differences in medium, inoculum and calculation make a direct comparison unsafe, but they cannot explain the contrast within our assay, where both phenotypes were tested side by side on the same day.

4.2. Copper: Inactive In Vitro, Not Necessarily in the Field

Copper sulfate did not halve the growth of any isolate at 100 μg mL^{-1}, and three isolates grew better on copper than on the control. We do not take that to mean copper is useless against frosty pod rot. Copper fungicides work on the plant surface, where ions released from the deposit kill spores before they germinate and penetrate. Their value is protective and multisite, and practical resistance in fungi is rare [16,55]. Established mycelium on a rich agar medium is a different target. Organic components of the medium can bind part of the copper, and growing hyphae tolerate concentrations that stop germinating spores. Our concentrations also refer to the pentahydrate salt, so 100 μg mL^{-1} of the salt supplied only about 25 μg mL^{-1} of Cu^{2+}, one more reason not to extrapolate the lack of effect in vitro to the field. Other Ecuadorian work found that copper sulfate inhibits *M. roreri* mycelium completely only at concentrations far above our range [13], and copper sprays remain useful partners

© 2026 by the author(s). Distributed under a Creative Commons CC BY license.

Preprints.org | NOT PEER-REVIEWED | Posted: 17 November 2026 https://doi.org/10.20944/preprints202611.1684.v1

of systemic fungicides in the field [12,14]. A copper baseline will have to come from spore germination assays over a wider range. In a resistance-management programme copper keeps its place precisely because it does not select at a single target site. The PCA put copper on its own axis, as one would expect if the copper response on agar is mostly noise.

4.3. Difenoconazole and Boscalid as Provisional Baselines

Difenoconazole and boscalid gave the narrow, unimodal distributions expected of populations that these fungicides have not yet selected [17,18]. Difenoconazole was the more active, in line with other systems in which it inhibits hyphal growth more strongly than strobilurins do [56], and with the good field performance of triazoles against *M. roreri* in Mexico [12]. Leaving aside three isolates with weak controls, all values fell within a roughly fourfold range below 2.3 μg mL^{-1}. When the control grows little, a small absolute reduction becomes a large relative one and the EC_{50} becomes unstable. Retesting them with vigorous inoculum will show whether their apparent tail reflects reduced sensitivity.

For both fungicides, 23 isolates already fix the P95 within a factor of about 1.5 and would reveal a twofold shift in the median with high power. The present data are good enough for a provisional baseline. Discriminatory concentrations of 1 μg mL^{-1} for difenoconazole and 5 μg mL^{-1} for boscalid would make practical screens. Any isolate that grows well at these concentrations deserves a full dose–response test and, later, sequencing of the target. SDHI resistance arises mainly from point mutations in *sdhB*, *sdhC* and *sdhD* [57–59]. DMI resistance comes from alterations or overexpression of *CYP51* and from enhanced efflux [60,61]. The genome of *M. roreri* [62] makes all of these genes accessible.

The moderate correlation between azoxystrobin and difenoconazole EC_{50} values ($\rho = 0.46$) is the part we cannot explain yet. The two fungicides have unrelated targets, and cross-resistance between them is not expected. A nonspecific mechanism such as increased efflux could lower sensitivity to several chemical classes at once [61]. Vigour differences could produce the same pattern. So could farm structure, because the two San Carlos isolates with the highest difenoconazole values (C16 and C17) were also less sensitive to azoxystrobin. The EC_{50} PCA did show a weak common sensitivity axis, but on its second axis difenoconazole and boscalid pulled in opposite directions, so there is no sign of general multidrug insensitivity. With 23 isolates from 16 field samples, we treat the correlation as a lead to follow up.

4.4. Farm Structure, Clonality and Implications for Monitoring and Rotation

M. roreri reproduces clonally [20], and its populations fall into genetic groups with strong geographic structure [6]. Our same-sample pairs fit that picture. For azoxystrobin they were far more alike than random pairs ($p = 0.001$), as one would expect if isolates from one sample are copies of one clone. The effective size of the collection is closer to 16 than to 23, and any analysis that treats the isolates as independent overstates precision, which is why our bootstrap resampled field samples. A less sensitive clone that arises or is selected on one farm can spread clonally within it, so that sensitivity becomes a property of farms. Three analyses agreed on that point. Farm was associated with the phenotypes and with the Ward clusters, and in the PCA it explained a significant part of the growth profile while cacao genotype and canton did not.

For monitoring, the answer differs by fungicide. Twenty-three isolates are enough for provisional baselines for difenoconazole and boscalid. For azoxystrobin they are not. The question there is no longer the shape of one distribution but the proportion of each phenotype, and the simulations show how poorly that proportion is known. A collection of about 120 isolates, stratified by farm and accompanied by spray records, would detect a threefold shift in the median with a power of 0.91–0.99 and would estimate the phenotype mix farm by farm. Detecting a twofold shift with a power of at least 0.8 would need a baseline near 320 isolates, compared with later samples of 100. A discriminatory concentration of 0.1 μg mL^{-1} would make such screening cheap. Where the two simulation methods diverged, in the tails, the divergence marks where more than 23 isolates are needed.

© 2026 by the author(s). Distributed under a Creative Commons CC BY license.

Preprints.org | NOT PEER-REVIEWED | Posted: 17 November 2026 https://doi.org/10.20944/preprints202611.1684.v1

Azoxystrobin, or any QoI, should not carry a programme against frosty pod rot on its own. On farms such as La Belleza we would use it sparingly until the less sensitive phenotype is explained. Where single-site fungicides are used, FRAC groups 3, 7 and 11 should be alternated or mixed, and QoI applications per season kept few. Pairing QoIs with copper, always alongside regular removal of diseased pods, would spread selection across more than one target [2,15,63]. The Mexican programmes that combined a single systemic application with monthly copper sprays [12] follow the same logic.

4.5. Future Work

Several open questions can be answered with the isolates already in the collection. For azoxystrobin, sequencing *cytb* in both phenotypes and testing azoxystrobin with SHAM on spores, as outlined above, will show whether a target-site change, alternative respiration or both lie behind the less sensitive phenotype. Spore germination assays will extend the work to the stage that QoIs and copper are meant to protect, and they will give copper the in vitro test that mycelium could not. We plan to repeat the boscalid assays for the low-vigour isolates C20, C22 and C23 with vigorous inoculum, and to confirm the identity of every isolate molecularly alongside the *cytb* work.

The farm structure raises a larger question. A farm-stratified collection of roughly 120 to 320 isolates across provinces, from the Amazon and the coast, would show whether the pattern we found in Orellana is general and would estimate the phenotype mix farm by farm. Including several farms of each cacao genotype would separate farm from cacao genotype, which the present collection was not designed to do. Application records were not kept on the sampled farms. From now on we will record the fungicide-use history of every sampled farm, noting which products are applied, boscalid and other SDHIs included, so that the less sensitive phenotype can be set against documented QoI exposure and the boscalid values against documented SDHI use. With that collection the PCA, now based on 23 isolates and 12 variables, can be refitted, and observed distributions can replace the simulated isolates and the single log-normal assumption behind the azoxystrobin power calculations. Field trials will then test the protectant role of copper and show how the in vitro phenotypes translate into disease control.

5. Conclusions

Among 23 isolates of *M. roreri* from Orellana, difenoconazole was the most active fungicide in mycelial growth assays, and boscalid gave a narrow distribution apart from three slow-growing isolates. Both data sets are usable as provisional baselines, with candidate discriminatory concentrations of 1 and 5 μg mL^{-1}. Copper sulfate was inactive on mycelium up to 100 μg mL^{-1}, which says little about its protectant value in the field. Azoxystrobin revealed two phenotypes about 30-fold apart. The less sensitive one was concentrated on a commercial CCN51 farm and a Nacional farm and was shared by isolates from the same field sample, and a PCA without prior grouping recovered the same farm-linked azoxystrobin axis. The pattern is consistent with a farm-level shift in QoI sensitivity that has spread clonally. The next step is to establish its mechanism and cause with SHAM and spore germination assays, *cytb* sequencing and spray records. Monitoring for azoxystrobin should sample by farm and enlarge the collection to about 120 isolates to detect a threefold shift, or to about 320 to detect a twofold shift against later samples of 100. A concentration of 0.1 μg mL^{-1} could be used to screen for the less sensitive phenotype.

Supplementary Materials: The following supporting information can be downloaded at the website of this paper posted on Preprints.org. Table S1: EC_{50} per isolate and fungicide, with model, bootstrap percentile and delta-method 95% confidence intervals, censoring, inhibition at each concentration and EC_{50} from the 120-h diameter; Table S2: AUMGC per isolate and concentration, with one-way ANOVA and Tukey groupings; Table S3: relative AUMGC by concentration for each fungicide (randomized complete block ANOVA and Tukey's test); Table S4: relative AUMGC of the four fungicides at each concentration (ANOVA, Tukey's test and Friedman test); Table S5: summary of the EC_{50} distributions; Table S6: simulation of 300 additional isolates (M1 and M2); Table S7:

© 2026 by the author(s). Distributed under a Creative Commons CC BY license.

Preprints.org | NOT PEER-REVIEWED | Posted: 17 November 2026 https://doi.org/10.20944/preprints202611.1684.v1

standardized EC_{50} values, cluster membership (Figure 5) and principal component scores and loadings (Figure 6); Table S8: raw colony diameters of all plates; Figures S1–S4: growth curves of each isolate for difenoconazole, boscalid, azoxystrobin and copper sulfate; File S1: R scripts used for the analyses (01_datos_ec50.R, 01b_bootstrap_ic.R, 02_abccm_medias.R, 03_poblacion.R, 04_dendrograma.R, 05_figuras.R, 05b_dendrograma_fig.R and 06_pca.R).

Author Contributions: Conceptualization, P.I.A.-R.; methodology, P.I.A.-R. and H.O.I.-R.; formal analysis, P.I.A.-R.; investigation, D.A.R.-R., V.B.M.-L. and N.C.T.-R.; resources, P.I.A.-R. and D.A.R.-R.; data curation, N.C.T.-R.; validation, A.F.T.A.F.e.F.; writing—original draft preparation, P.I.A.-R.; writing—review and editing, A.F.T.A.F.e.F., D.A.R.-R., V.B.M.-L., N.C.T.-R. and H.O.I.-R.; supervision, P.I.A.-R. All authors have read and agreed to the published version of the manuscript.

Funding: This study was supported by the Research Project "IDIPIM-002—Implementación de una Plataforma Informática de Alertas Tempranas Fitosanitarias Agrícolas en los cantones La Joya de los Sachas, Loreto y Francisco de Orellana" funded by the Escuela Superior Politécnica de Chimborazo through its Research Deanship (Decanato de Investigación, DDI-ESPOCH).

Institutional Review Board Statement: Not applicable.

Informed Consent Statement: Not applicable.

Data Availability Statement: The raw colony measurements of all plates (Table S8) and the R scripts used for the analyses (File S1) are provided as Supplementary Materials.

Acknowledgments: The authors thank the Escuela Superior Politécnica de Chimborazo, since this study is part of the Project "IDIPIM-002—Implementación de una Plataforma Informática de Alertas Tempranas Fitosanitarias Agrícolas en los cantones La Joya de los Sachas, Loreto y Francisco de Orellana". We also thank the cacao growers of Joya de los Sachas, Francisco de Orellana and Loreto who allowed sampling on their farms.

Conflicts of Interest: The authors declare no conflicts of interest.

References

1. Phillips-Mora, W.; Wilkinson, M.J. Frosty Pod of Cacao: A Disease with a Limited Geographic Range but Unlimited Potential for Damage. *Phytopathology* **2007**, *97*, 1644–1647. https://doi.org/10.1094/PHYTO-97-12-1644
2. Bailey, B.A.; Evans, H.C.; Phillips-Mora, W.; Ali, S.S.; Meinhardt, L.W. *Moniliophthora roreri*, Causal Agent of Cacao Frosty Pod Rot. *Mol. Plant Pathol.* **2018**, *19*, 1580–1594. https://doi.org/10.1111/mpp.12648
3. Evans, H.C.; Stalpers, J.A.; Samson, R.A.; Benny, G.L. On the Taxonomy of *Monilia roreri*, an Important Pathogen of *Theobroma cacao* in South America. *Can. J. Bot.* **1978**, *56*, 2528–2532. https://doi.org/10.1139/b78-305
4. Aime, M.C.; Phillips-Mora, W. The Causal Agents of Witches' Broom and Frosty Pod Rot of Cacao (Chocolate, *Theobroma cacao*) Form a New Lineage of Marasmiaceae. *Mycologia* **2005**, *97*, 1012–1022. https://doi.org/10.3852/mycologia.97.5.1012
5. Díaz-Valderrama, J.R.; Leiva-Espinoza, S.T.; Aime, M.C. The History of Cacao and Its Diseases in the Americas. *Phytopathology* **2020**, *110*, 1604–1619. https://doi.org/10.1094/PHYTO-05-20-0178-RVW
6. Phillips-Mora, W.; Aime, M.C.; Wilkinson, M.J. Biodiversity and Biogeography of the Cacao (*Theobroma cacao*) Pathogen *Moniliophthora roreri* in Tropical America. *Plant Pathol.* **2007**, *56*, 911–922. https://doi.org/10.1111/j.1365-3059.2007.01646.x
7. Zarrillo, S.; Gaikwad, N.; Lanaud, C.; Powis, T.; et al. The Use and Domestication of *Theobroma cacao* during the Mid-Holocene in the Upper Amazon. *Nat. Ecol. Evol.* **2018**, *2*, 1879–1888. https://doi.org/10.1038/s41559-018-0697-x
8. Motamayor, J.C.; Lachenaud, P.; da Silva e Mota, J.W.; Loor, R.; Kuhn, D.N.; Brown, J.S.; Schnell, R.J. Geographic and Genetic Population Differentiation of the Amazonian Chocolate Tree (*Theobroma cacao* L). *PLoS ONE* **2008**, *3*, e3311. https://doi.org/10.1371/journal.pone.0003311

© 2026 by the author(s). Distributed under a Creative Commons CC BY license.

Preprints.org | NOT PEER-REVIEWED | Posted: 17 November 2026 https://doi.org/10.20944/preprints202611.1684.v1

9. Alvarez-Romero, P.I.; Román-Robalino, D.A.; Salazar-Castañeda, E.P.; Suárez-Cedillo, S.E.; Hinojosa-Sánchez, L.A.; Ferreira, A.F.T.A.F.e.; Guallpa-Calva, M.A. Diversity and Composition of Endophytic Fungal Communities Associated with Cocoa (*Theobroma cacao* L.) Fruits in the Northern Ecuadorian Amazon. *Int. J. Plant Biol.* **2025**, *16*, 17. https://doi.org/10.3390/ijpb16010017
10. Krauss, U.; Soberanis, W. Rehabilitation of Diseased Cacao Fields in Peru through Shade Regulation and Timing of Biocontrol Measures. *Agrofor. Syst.* **2001**, *53*, 179–184. https://doi.org/10.1023/A:1013376504268
11. Leandro-Muñoz, M.E.; Tixier, P.; Germon, A.; Rakotobe, V.; Phillips-Mora, W.; Maximova, S.; Avelino, J. Effects of Microclimatic Variables on the Symptoms and Signs Onset of *Moniliophthora roreri*, Causal Agent of Moniliophthora Pod Rot in Cacao. *PLoS ONE* **2017**, *12*, e0184638. https://doi.org/10.1371/journal.pone.0184638
12. Torres-de-la-Cruz, M.; Quevedo-Damián, I.; Ortiz-García, C.F.; Lagúnez-Espinoza, L.C.; Nieto-Angel, D.; Pérez-de la Cruz, M. Control Químico de *Moniliophthora roreri* en México. *Biotecnia* **2019**, *21*, 55–61.
13. Amaya-Márquez, D.J.; Avilés Párraga, D.D.; Peñaherrera-Morales, A.L.; Mendoza Thompson, J.U.; Sánchez Castro, E.E.; Álava Murillo, A.G. In Vitro Evaluation of Chemical Fungicides for the Control of *Moniliophthora roreri*, the Causal Agent of Cacao Frosty Pod Rot (*Theobroma cacao* L.). *Rev. Tecnol. ESPOL* **2025**, *37*, 132–143. https://doi.org/10.37815/rte.v37n2.1325
14. Amaya-Márquez, D.; Barreto-Macias, A.; Farah-Asang, S.; García Ortega, Y.; Peñaherrera-Morales, A.; Avilés Párraga, D.; Calle Romero, K. Incidence of *Moniliophthora roreri* Pathogen of Cocoa in Ecuador and Chemical Management at In Vitro and In Vivo Levels. *Sci. Agropecu.* **2026**, *17*, 257–267. https://doi.org/10.17268/sci.agropecu.2026.018
15. FRAC. *FRAC Code List 2024: Fungal Control Agents Sorted by Cross-Resistance Pattern and Mode of Action (Including Coding for FRAC Groups on Product Labels)*; Fungicide Resistance Action Committee, CropLife International: Brussels, Belgium, 2024. Available online: https://www.frac.info (accessed on 1 November 2026).
16. Brent, K.J.; Hollomon, D.W. *Fungicide Resistance in Crop Pathogens: How Can It Be Managed?*, 2nd revised ed.; FRAC Monograph No. 1; Fungicide Resistance Action Committee, CropLife International: Brussels, Belgium, 2007; ISBN 90-72398-07-6.
17. Russell, P.E. *Sensitivity Baselines in Fungicide Resistance Research and Management*; FRAC Monograph No. 3; Fungicide Resistance Action Committee, CropLife International: Brussels, Belgium, 2004.
18. Lucas, J.A.; Hawkins, N.J.; Fraaije, B.A. The Evolution of Fungicide Resistance. *Adv. Appl. Microbiol.* **2015**, *90*, 29–92. https://doi.org/10.1016/bs.aambs.2014.09.001
19. Espinoza-Lozano, F.; Amaya-Márquez, D.; Pinto, C.M.; Villavicencio-Vásquez, M.; Sosa del Castillo, D.; Pérez-Martínez, S. Multiple Introductions of *Moniliophthora roreri* from the Amazon to the Pacific Region in Ecuador and Shared High Azoxystrobin Sensitivity. *Agronomy* **2022**, *12*, 1119. https://doi.org/10.3390/agronomy12051119
20. Díaz-Valderrama, J.R.; Aime, M.C. The Cacao Pathogen *Moniliophthora roreri* (Marasmiaceae) Possesses Bi-allelic A and B Mating Loci but Reproduces Clonally. *Heredity* **2016**, *116*, 491–501. https://doi.org/10.1038/hdy.2016.5
21. Castellani, A. The "Water Cultivation" of Pathogenic Fungi. *J. Trop. Med. Hyg.* **1963**, *66*, 283–284.
22. Urzì, C.; De Leo, F. Sampling with Adhesive Tape Strips: An Easy and Rapid Method to Monitor Microbial Colonization on Monument Surfaces. *J. Microbiol. Methods* **2001**, *44*, 1–11.
23. Mihajlović, M.; Rekanović, E.; Hrustić, J.; Grahovac, M.; Tanović, B. In Vitro and In Vivo Toxicity of Fungicides and Biofungicides for the Control of Verticillium and Fusarium Wilt of Pepper. *Pestic. Fitomed.* **2021**, *36*, 23–34. https://doi.org/10.2298/PIF2101023M
24. Shaner, G.; Finney, R.E. The Effect of Nitrogen Fertilization on the Expression of Slow-Mildewing Resistance in Knox Wheat. *Phytopathology* **1977**, *67*, 1051–1056. https://doi.org/10.1094/Phyto-67-1051
25. Ritz, C.; Baty, F.; Streibig, J.C.; Gerhard, D. Dose-Response Analysis Using R. *PLoS ONE* **2015**, *10*, e0146021. https://doi.org/10.1371/journal.pone.0146021
26. Wood, P.M.; Hollomon, D.W. A Critical Evaluation of the Role of Alternative Oxidase in the Performance of Strobilurin and Related Fungicides Acting at the Qo Site of Complex III. *Pest Manag. Sci.* **2003**, *59*, 499–511. https://doi.org/10.1002/ps.655

© 2026 by the author(s). Distributed under a Creative Commons CC BY license.

Preprints.org | NOT PEER-REVIEWED | Posted: 17 November 2026 https://doi.org/10.20944/preprints202611.1684.v1

27. Alves, K.S. *ec50estimator: An Automated Way to Estimate EC50 for Stratified Datasets*, R Package Version 1.0.0; 2026. Available online: https://CRAN.R-project.org/package=ec50estimator (accessed on 1 November 2026).
28. Gudmestad, N.C.; Arabiat, S.; Miller, J.S.; Pasche, J.S. Prevalence and Impact of SDHI Fungicide Resistance in *Alternaria solani*. *Plant Dis.* **2013**, *97*, 952–960. https://doi.org/10.1094/PDIS-12-12-1176-RE
29. Edgington, L.V.; Khew, K.L.; Barron, G.L. Fungitoxic Spectrum of Benzimidazole Compounds. *Phytopathology* **1971**, *61*, 42–44. https://doi.org/10.1094/Phyto-61-42
30. Helsel, D.R. *Statistics for Censored Environmental Data Using Minitab and R*, 2nd ed.; John Wiley & Sons: Hoboken, NJ, USA, 2012.
31. Therneau, T.M.; Grambsch, P.M. *Modeling Survival Data: Extending the Cox Model*; Springer: New York, NY, USA, 2000. https://doi.org/10.1007/978-1-4757-3294-8
32. Field, C.A.; Welsh, A.H. Bootstrapping Clustered Data. *J. R. Stat. Soc. Ser. B Stat. Methodol.* **2007**, *69*, 369–390. https://doi.org/10.1111/j.1467-9868.2007.00593.x
33. Efron, B.; Tibshirani, R.J. *An Introduction to the Bootstrap*; Chapman & Hall: New York, NY, USA, 1993.
34. Holm, S. A Simple Sequentially Rejective Multiple Test Procedure. *Scand. J. Stat.* **1979**, *6*, 65–70.
35. Benaglia, T.; Chauveau, D.; Hunter, D.R.; Young, D.S. mixtools: An R Package for Analyzing Finite Mixture Models. *J. Stat. Softw.* **2009**, *32*, 1–29. https://doi.org/10.18637/jss.v032.i06
36. McLachlan, G.J. On Bootstrapping the Likelihood Ratio Test Statistic for the Number of Components in a Normal Mixture. *J. R. Stat. Soc. Ser. C Appl. Stat.* **1987**, *36*, 318–324. https://doi.org/10.2307/2347790
37. Ward, J.H., Jr. Hierarchical Grouping to Optimize an Objective Function. *J. Am. Stat. Assoc.* **1963**, *58*, 236–244.
38. Rousseeuw, P.J. Silhouettes: A Graphical Aid to the Interpretation and Validation of Cluster Analysis. *J. Comput. Appl. Math.* **1987**, *20*, 53–65. https://doi.org/10.1016/0377-0427(87)90125-7
39. Hennig, C. Cluster-Wise Assessment of Cluster Stability. *Comput. Stat. Data Anal.* **2007**, *52*, 258–271.
40. Jolliffe, I.T.; Cadima, J. Principal Component Analysis: A Review and Recent Developments. *Phil. Trans. R. Soc. A* **2016**, *374*, 20150202. https://doi.org/10.1098/rsta.2015.0202
41. Anderson, M.J. A New Method for Non-Parametric Multivariate Analysis of Variance. *Austral Ecol.* **2001**, *26*, 32–46. https://doi.org/10.1111/j.1442-9993.2001.01070.pp.x
42. Silverman, B.W. *Density Estimation for Statistics and Data Analysis*; Monographs on Statistics and Applied Probability 26; Chapman and Hall: London, UK, 1986.
43. R Core Team. *R: A Language and Environment for Statistical Computing*; R Foundation for Statistical Computing: Vienna, Austria, 2024. Available online: https://www.R-project.org/ (accessed on 1 November 2026).
44. de Mendiburu, F. *agricolae: Statistical Procedures for Agricultural Research*, R Package Version 1.3-7; 2023. Available online: https://CRAN.R-project.org/package=agricolae (accessed on 1 November 2026).
45. Wickham, H. *ggplot2: Elegant Graphics for Data Analysis*; Springer: New York, NY, USA, 2016. https://doi.org/10.1007/978-3-319-24277-4
46. Bartlett, D.W.; Clough, J.M.; Godwin, J.R.; Hall, A.A.; Hamer, M.; Parr-Dobrzanski, B. The Strobilurin Fungicides. *Pest Manag. Sci.* **2002**, *58*, 649–662. https://doi.org/10.1002/ps.520
47. Gisi, U.; Sierotzki, H.; Cook, A.; McCaffery, A. Mechanisms Influencing the Evolution of Resistance to Qo Inhibitor Fungicides. *Pest Manag. Sci.* **2002**, *58*, 859–867. https://doi.org/10.1002/ps.565
48. Fernández-Ortuño, D.; Torés, J.A.; de Vicente, A.; Pérez-García, A. Mechanisms of Resistance to QoI Fungicides in Phytopathogenic Fungi. *Int. Microbiol.* **2008**, *11*, 1–9. https://doi.org/10.2436/20.1501.01.38
49. Sierotzki, H.; Frey, R.; Wullschleger, J.; Palermo, S.; Karlin, S.; Godwin, J.; Gisi, U. Cytochrome *b* Gene Sequence and Structure of *Pyrenophora teres* and *P. tritici-repentis* and Implications for QoI Resistance. *Pest Manag. Sci.* **2007**, *63*, 225–233. https://doi.org/10.1002/ps.1279
50. Grasso, V.; Palermo, S.; Sierotzki, H.; Garibaldi, A.; Gisi, U. Cytochrome *b* Gene Structure and Consequences for Resistance to Qo Inhibitor Fungicides in Plant Pathogens. *Pest Manag. Sci.* **2006**, *62*, 465–472.
51. Formighieri, E.F.; Tiburcio, R.A.; Armas, E.D.; Medrano, F.J.; Shimo, H.; Carels, N.; Góes-Neto, A.; Cotomacci, C.; Carazzolle, M.F.; Sardinha-Pinto, N.; et al. The Mitochondrial Genome of the Phytopathogenic Basidiomycete *Moniliophthora perniciosa* Is 109 kb in Size and Contains a Stable Integrated Plasmid. *Mycol. Res.* **2008**, *112*, 1136–1152. https://doi.org/10.1016/j.mycres.2008.04.014

© 2026 by the author(s). Distributed under a Creative Commons CC BY license.

Preprints.org | NOT PEER-REVIEWED | Posted: 17 November 2026 https://doi.org/10.20944/preprints202611.1684.v1

52. Costa, G.G.L.; Cabrera, O.G.; Tiburcio, R.A.; Medrano, F.J.; Carazzolle, M.F.; Thomazella, D.P.T.; Schuster, S.C.; Carlson, J.E.; Guiltinan, M.J.; Bailey, B.A.; et al. The Mitochondrial Genome of *Moniliophthora roreri*, the Frosty Pod Rot Pathogen of Cacao. *Fungal Biol.* **2012**, *116*, 551–562. https://doi.org/10.1016/j.funbio.2012.01.008
53. Thomazella, D.P.T.; Teixeira, P.J.P.L.; Oliveira, H.C.; Saviani, E.E.; Rincones, J.; Toni, I.M.; Reis, O.; Garcia, O.; Meinhardt, L.W.; Salgado, I.; Pereira, G.A.G. The Hemibiotrophic Cacao Pathogen *Moniliophthora perniciosa* Depends on a Mitochondrial Alternative Oxidase for Biotrophic Development. *New Phytol.* **2012**, *194*, 1025–1034. https://doi.org/10.1111/j.1469-8137.2012.04119.x
54. Mondal, S.N.; Bhatia, A.; Shilts, T.; Timmer, L.W. Baseline Sensitivities of Fungal Pathogens of Fruit and Foliage of Citrus to Azoxystrobin, Pyraclostrobin, and Fenbuconazole. *Plant Dis.* **2005**, *89*, 1186–1194. https://doi.org/10.1094/PD-89-1186
55. Lamichhane, J.R.; Osdaghi, E.; Behlau, F.; Köhl, J.; Jones, J.B.; Aubertot, J.-N. Thirteen Decades of Antimicrobial Copper Compounds Applied in Agriculture. A Review. *Agron. Sustain. Dev.* **2018**, *38*, 28. https://doi.org/10.1007/s13593-018-0503-9
56. Reuveni, M.; Sheglov, D. Effects of Azoxystrobin, Difenoconazole, Polyoxin B (Polar) and Trifloxystrobin on Germination and Growth of *Alternaria alternata* and Decay in Red Delicious Apple Fruit. *Crop Prot.* **2002**, *21*, 951–955. https://doi.org/10.1016/S0261-2194(02)00073-X
57. Avenot, H.F.; Sellam, A.; Karaoglanidis, G.; Michailides, T.J. Characterization of Mutations in the Iron-Sulphur Subunit of Succinate Dehydrogenase Correlating with Boscalid Resistance in *Alternaria alternata* from California Pistachio. *Phytopathology* **2008**, *98*, 736–742. https://doi.org/10.1094/PHYTO-98-6-0736
58. Avenot, H.F.; Michailides, T.J. Progress in Understanding Molecular Mechanisms and Evolution of Resistance to Succinate Dehydrogenase Inhibiting (SDHI) Fungicides in Phytopathogenic Fungi. *Crop Prot.* **2010**, *29*, 643–651. https://doi.org/10.1016/j.cropro.2010.02.019
59. Sierotzki, H.; Scalliet, G. A Review of Current Knowledge of Resistance Aspects for the Next-Generation Succinate Dehydrogenase Inhibitor Fungicides. *Phytopathology* **2013**, *103*, 880–887. https://doi.org/10.1094/PHYTO-01-13-0009-RVW
60. Price, C.L.; Parker, J.E.; Warrilow, A.G.S.; Kelly, D.E.; Kelly, S.L. Azole Fungicides—Understanding Resistance Mechanisms in Agricultural Fungal Pathogens. *Pest Manag. Sci.* **2015**, *71*, 1054–1058. https://doi.org/10.1002/ps.4029
61. Hu, M.; Chen, S. Non-Target Site Mechanisms of Fungicide Resistance in Crop Pathogens: A Review. *Microorganisms* **2021**, *9*, 502. https://doi.org/10.3390/microorganisms9030502
62. Meinhardt, L.W.; Costa, G.G.L.; Thomazella, D.P.T.; Teixeira, P.J.P.L.; Carazzolle, M.F.; Schuster, S.C.; et al. Genome and Secretome Analysis of the Hemibiotrophic Fungal Pathogen, *Moniliophthora roreri*, Which Causes Frosty Pod Rot Disease of Cacao: Mechanisms of the Biotrophic and Necrotrophic Phases. *BMC Genomics* **2014**, *15*, 164. https://doi.org/10.1186/1471-2164-15-164
63. Corkley, I.; Fraaije, B.; Hawkins, N. Fungicide Resistance Management: Maximizing the Effective Life of Plant Protection Products. *Plant Pathol.* **2022**, *71*, 150–169. https://doi.org/10.1111/ppa.13467

Disclaimer/Publisher's Note: The statements, opinions and data contained in all publications are solely those of the individual author(s) and contributor(s) and not of MDPI and/or the editor(s). MDPI and/or the editor(s) disclaim responsibility for any injury to people or property resulting from any ideas, methods, instructions or products referred to in the content.

© 2026 by the author(s). Distributed under a Creative Commons CC BY license.